Supporting Information

Decanuclear Fe^{III} clusters with hemiacetal ligands: a new {M$_{10}$(μ$_3$-O)$_8$} cluster core.

Júlia Mayans,[‡] Laura Roc,[‡] Mercè Font-Bardia,[#] Albert Escuer,[*,‡]

[‡] Departament de Química Inorgànica i Orgànica, Secció Inorgànica and Institut de Nanociència i Nanotecnologia (IN²UB), Universitat de Barcelona, Martí i Franqués 1-11, Barcelona-08028, Spain.

[#] Departament de Mineralogia, Cristal·lografia i Dipòsits Minerals, Universitat de Barcelona, Martí Franqués s/n, 08028 Barcelona (Spain) and Unitat de Difracció de R-X. Centre Científic i Tecnològic de la Universitat de Barcelona (CCiTUB), Solé i Sabarís 1-3. 08028 Barcelona.

Experimental

Physical measurements: Magnetic susceptibility measurements were carried out on polycrystalline samples with a MPMS5 Quantum Design susceptometer working in the range 30-300 K under magnetic fields of 0.3 T and under a field of 0.03T in the 30 – 2 K range to avoid saturation effects at low temperature. Diamagnetic corrections were estimated from Pascal Tables. Infrared spectra (4000-400 cm^{-1}) were recorded from KBr pellets on a Bruker IFS-125 FT-IR spectrophotometer. Powder X-ray diffraction was performed with a PANalytical X'Pert PRO MPD θ/θ powder diffractometer of 240 millimetres of radius, in a configuration of convergent beam with a focalizing mirror and a transmission geometry with flat samples sandwiched between low absorbing films and Cu Kα radiation (λ = 1.5418 Å).

Synthetic procedure.

N,N'-Bis-[pyridin-2-ylmethylene]cyclo-hexane-1,2-diamine (L1): The Schiff bases were prepared mixing a solution of 2-pyridinecarboxaldehyde (1.0 mmol,) and the corresponding diaminociclohexane (*R,R*) or (*S, S*) isomer (0.5 mmol) in 10 mL of methanol and stirring for 2 hours at room temperature. The resulting solution was directly employed for the further synthesis but the ligand can be isolated as a white solid removing the solvent and recrystallizing in diethylether.

Synthesis from the Schiff base **L1**:

[Fe$_{10}$(MeO-hmp$^-$)$_8$(NO$_3^-$)$_6$(SCN$^-$)$_2$(μ$_3$-O)$_6$(μ$_3$-OH)$_2$]·CH$_2$Cl$_2$·9H$_2$O (1·CH$_2$Cl$_2$·9H$_2$O):
NaSCN (0.081 g, 1 mmol) and a the previously prepared solution of L1 (0.5 mmol) were added to a methanolic solution (5 mL) of Fe(NO$_3$)$_3$·9H$_2$O (0.404 g, 1 mmol). The dark red solution was

stirred for 30 minutes and layered with diethylether. A crop of well formed red crystals were obtained after one week in a 30% yield.

[Fe$_{10}$(MeO-hmp$^-$)$_8$(NO$_3$$^-$)$_7$($\mu_3$-O)$_7$($\mu_3$-OH)]·0.625MeOH (**2**·0.625MeOH). Following the same procedure but without the addition of NaSCN an orange-reddish solution was obtained. Layering the solution with diethylether, red crystals were obtained in few days.

Synthesis from **pyridinecarboxaldehydes**:

In light of the structural characterization that evidences the hydrolysis of the Schiff base, the complexes **1 - 3** were synthesized by direct reaction from the corresponding aldehydes.

[Fe$_{10}$(MeO-hmp$^-$)$_8$(NO$_3$$^-$)$_6$(SCN$^-$)$_2$($\mu_3$-O)$_6$($\mu_3$-OH)$_2$]·CH$_2Cl_2$·9H$_2$O (**1**·CH$_2Cl_2$·9H$_2$O) from 2-pyridinecarboxaldehyde:

compound **1** was prepared by the reaction of 2-pyridinecarboxaldehyde (0.213 g, 1mmol), Fe(NO$_3$)$_3$·9H$_2$O (0.202 g, 0.5 mmol), NaSCN (0.081 g, 1 mmol) and Et$_3$N (0.05 g, 0.5 mmol) in 15 mL of MeOH. The dark red solution was stirred for 30 min, mixed with 10 mL of dichloromethane and layered with diethylether. Well formed red crystals were obtained after one week in *circa* 30% yield. Anal. calculated/found (%) for the complex formula: **1**, C, 30.53/29.9; H 2.92/3.3; N 9.82/9.4; S 2.81/2.7.

[Fe$_{10}$(MeO-hmp$^-$)$_8$(NO$_3$$^-$)$_7$($\mu_3$-O)$_7$($\mu_3$-OH)]·0.625MeOH (**2**·0.625MeOH) and **[Fe$_{10}$(MeO-3Mehmp$^-$)$_8$(NO$_3$$^-$)$_8$($\mu_3$-O)$_6$($\mu_3$-OH)$_2$]·solvents** (**3**·solvents): the two complexes were obtained following the same procedure. The clusters were prepared by the reaction of 2-pyridinecarboxaldehyde (0.213 g, 1mmol) for **2** or 3-methylpyridine-2-carboxaldehyde (0.061 g, 0.5 mmol) for **3**, Fe(NO$_3$)$_3$·9H$_2$O (0.202 g, 0.5 mmol) and Et$_3$N (0.05 g, 0.5 mmol), in 15 mL of MeOH. The orange-red solutions were stirred for 30 min and layered with diethylether. Orange-reddish crystals were obtained after one week in a 25% yield. Anal. calculated/found (%) for the complex formula: **2**, C, 30.21/30.1; H 2.94/3.2; N 9.44/9.2; **3**, C, 29.35/28.1; H 2.99/3.1; N 9.78/9.9
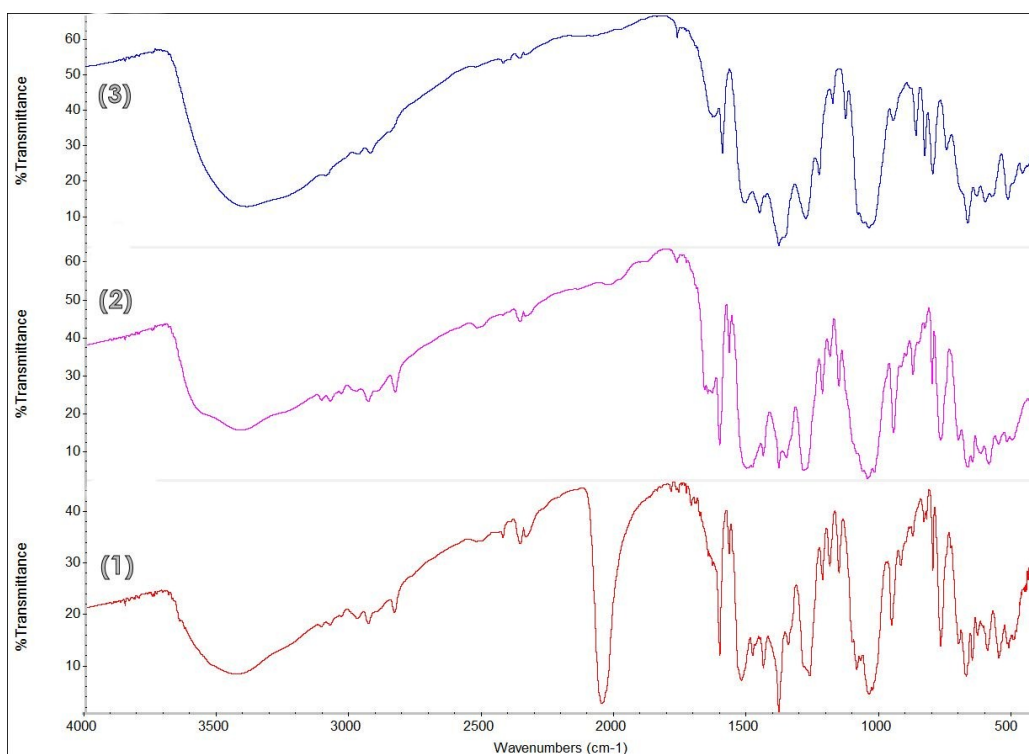
Figure S1. IR spectra for complexes **1**(red), **2** (violet) and **3** (blue). As should be expected the three spectra are very similar with the exception of the intense thiocyanate CN stretching at 2050 cm^{-1}.

Complementary information about unsuccessful syntheses:

-The same reaction that allows to complex **1** with sodium azide instead thyocyanate or the reactions parallel to **2** and **3** starting from 6-methyl-2-pyidylaldehyde or 2-quinolilaldehyde were tried but crystalline products were not obtained.
-Reaction of the enantiomerically pure ligand (*R*)-2-(1-hydroxyethyl)pyridine with iron(III) nitrate do not allows to characterizable products.
-Reactions with other alcohols such ethanol or propanol do not allow to characterizable products.

Crystal structure reports

The X-ray intensity data were measured on a D8 Venture system equipped with a multilayer monochromator and a Mo microfocus (λ = 0.71073 Å). The frames were integrated with the Bruker SAINT software package using a narrow-frame algorithm. The structures were solved and refined using the Bruker SHELXTL Software Package.

The quality of the structure of compound **1** was not satisfactory from crystallographic point of view. The bond parameters for the nitrate ligands around N9 are adequate and maintaining the charge balance, suggest a partial disorder with SCN$^-$. As information for the reader, the structure was deposited at the CCDC database as *CSD Communication* (CCDC number 1896201).

Compound **1**: A red needle-like specimen of $C_{58}H_{61}Cl_0Fe_{10}N_{16}O_{42}S_2$, approximate dimensions 0.062 mm x 0.090 mm x 0.382 mm, was used for the X-ray crystallographic analysis. The integration of the data using a tetragonal unit cell yielded a total of 60930 reflections to a maximum θ angle of 26.40° (0.80 Å resolution), of which 18056 were independent (average redundancy 3.375, completeness = 99.8%, R_{int} = 8.22%, R_{sig} = 8.23%) and 14215 (78.73%) were greater than $2\sigma(F^2)$. The final cell constants of $\underline{a}$ = 23.6460(9) Å, $\underline{b}$ = 23.6460(9) Å, $\underline{c}$ = 16.0842(6) Å, volume = 8993.2(8) Å^3, are based upon the refinement of the XYZ-centroids of 9936 reflections above 20 σ(I) with 4.609° < 2θ < 52.43°. Data were corrected for absorption effects using the multi-scan method (SADABS). The ratio of minimum to maximum apparent transmission was 0.792. The calculated minimum and maximum transmission coefficients (based on crystal size) are 0.6072 and 0.7450.

The structure was solved and refined using the space group P 42, with Z = 4 for the formula unit, $C_{58}H_{61}Cl_0Fe_{10}N_{16}O_{42}S_2$. The final anisotropic full-matrix least-squares refinement on F^2 with 1116 variables converged at R1 = 7.18%, for the observed data and wR2 = 16.41% for all data. The goodness-of-fit was 1.064. The largest peak in the final difference electron density synthesis was 1.373 e$^-$/Å^3 and the largest hole was -1.269 e$^-$/Å^3 with an RMS deviation of 0.132 e$^-$/Å^3. On the basis of the final model, the calculated density was 1.682 g/cm^3 and F(000), 4596 e$^-$.

Compound **2**: A red prism-like specimen of $C_{56.62}H_{66.75}Fe_{10}N_{15}O_{45.62}$, approximate dimensions 0.055 mm x 0.106 mm x 0.166 mm, was used for the X-ray crystallographic analysis.

The integration of the data using a triclinic unit cell yielded a total of 25280 reflections to a maximum θ angle of 30.09° (0.71 Å resolution), of which 25280 were independent (average redundancy 1.000, completeness = 99.7%, R_{int} = 9.91%, R_{sig} = 5.45%) and 17392 (68.80%) were greater than $2\sigma(F^2)$. The final cell constants of $\underline{a}$ = 13.3894(8)Å, $\underline{b}$ = 14.6630(8) Å, $\underline{c}$ = 24.6137(14) Å, α = 77.019(2)°, β = 82.090(2)°, γ = 66.598(2)°, volume = 4315.2(4) Å^3, are based upon the refinement of the XYZ-centroids of reflections above 20 σ(I). Data were corrected for absorption effects using the Multi-Scan method (SADABS). The calculated minimum and maximum transmission coefficients (based on crystal size) are 0.6873 and 0.7460.

The structure was solved and refined using the space group P -1, with Z = 1 for the formula unit, $C_{113.25}H_{135}Fe_{20}N_{30}O_{91.25}$. The final anisotropic full-matrix least-squares refinement on F^2 with 1173 variables converged at R1 = 3.76%, for the observed data and wR2 = 10.97% for all data. The goodness-of-fit was 1.013. The largest peak in the final difference electron density synthesis was 1.068e$^-$/Å^3 and the largest hole was -0.959 e$^-$/Å^3 with an RMS deviation of 0.096 e$^-$/Å^3. On the basis of the final model, the calculated density was 1.729 g/cm^3 and F(000), 2273 e$^-$.

Compound **3**: A red prism-like specimen of $C_{64}H_{76}Fe_{10}N_{16}O_{40}$, approximate dimensions 0.149 mm x 0.152 mm x 0.186 mm, was used for the X-ray crystallographic analysis. The frames were integrated with the Bruker SAINT software package using a narrow-frame algorithm. The integration of the data using a tetragonal unit cell yielded a total of 27264 reflections to a maximum θ angle of 23.26° (0.90 Å resolution), of which 3869 were independent (average redundancy 7.047, completeness = 99.6%, R_{int} = 10.08%, R_{sig} = 6.68%) and 2999 (77.51%) were greater than $2\sigma(F^2)$. The final cell constants of $\underline{a}$ = 18.180(4) Å, $\underline{b}$ = 18.180(4) Å, $\underline{c}$ = 16.360(4) Å, volume = 5407.(2) Å^3, are based upon the refinement of the XYZ-centroids of reflections above 20 σ(I). Data were corrected for absorption

effects using the Multi-Scan method (SADABS). The calculated minimum and maximum transmission coefficients (based on crystal size) are 0.5521 and 0.7449.

The structure was solved and refined using the space group I -4, with Z = 2 for the formula unit, $C_{64}H_{76}Fe_{10}N_{16}O_{48}$. The final anisotropic full-matrix least-squares refinement on F^2 with 221 variables converged at R1 = 7.82%, for the observed data and wR2 = 23.09% for all data. The goodness-of-fit was 1.169. The largest peak in the final difference electron density synthesis was 1.542 e$^-$/Å^3 and the largest hole was -0.743 e$^-$/Å^3 with an RMS deviation of 0.135 e$^-$/Å^3. On the basis of the final model, the calculated density was 1.472 g/cm^3 and F(000), 2432 e$^-$.
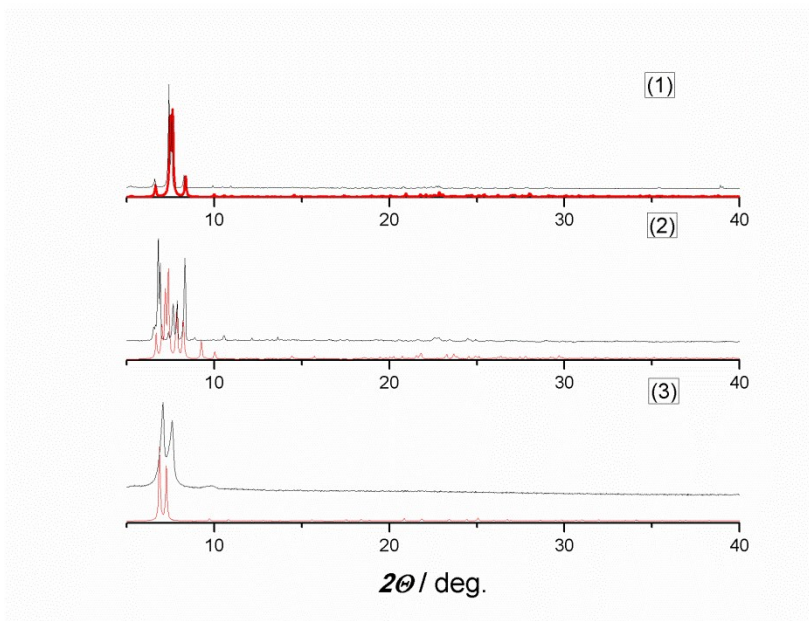

Figure S2. Powder diffraction spectra for the powdered samples of complexes **1-3** employed for the instrumental measurements. The small differences in the position of the peaks are attributable to changes in the cell parameters derived from the loss of crystallization solvents during the preparation of the samples (the crystals show fast degradation at open air).

Table S1. Crystal data and structure refinement for coordination compounds **1** (partial resolution), **2** and **3**.

	1	2	3
Formula	$[C_{233}H_{268}Cl_2Fe_{40}N_{64}O_{170}S_8]$	$[C_{113.25}H_{135}Fe_{20}N_{30}O_{91.25}]$	$C_{64}H_{76}Fe_{10}N_{16}O_{40}$
FW	9246.48	4493.50	2395.90
System	Tetragonal	Triclinic	Tetragonal
Space group	P42	P -1	I-4
$a/Å$	23.6462(9)	13.3894(8)	18.180(4)
$b/Å$	23.6462(9)	14.6630(8)	18.180(4)
$c/Å$	16.0848(6)	24.614(1)	16.360(4)
α/**deg.**	90	77.019(2)	90
β/**deg.**	90	82.090(2)	90
γ/**deg.**	90	66.598(2)	90
$V/Å^3$	8993.7(8)	4315.2(4)	5407.2
Z	1	1	2
T, **K**	100(2)	100(2)	100(2)
ρ_{calc}, **g.cm-3**	1.707	1.729	1.472
μ **(MoK), mm-1**	1.722	1.732	1.389
R	0.0475	0.0376	0.0782
ωR^2	0.00863	0.0973	0.1964

Table S2. Bond distances and angles for compound **2**.

Distance (Å)		Angle (deg.)	
Fe-N (pyridyl)		**μ-O (from MeOhmp⁻)**	
Fe(1)-N(1)	2.137(2)	Fe(1)-O(1)-Fe(2)	98.60(8)
Fe(1)-N(2)	2.159(2)	Fe(1)-O(3)-Fe(9)	95.81(7)
Fe(3)-N(3)	2.130(2)	Fe(2)-O(4)-Fe(3)	100.38(7)
Fe(3)-N(4)	2.144(2)	Fe(3)-O(7)-Fe(4)	95.23(7)
Fe(5)-N(5)	2.143(2)	Fe(5)-O(9)-Fe(10)	94.16(7)
Fe(5)-N(6)	2.158(2)	Fe(5)-O(11)-Fe(6)	95.58(7)
Fe(7)-N(8)	2.140(3)	Fe(6)-O(13)-Fe(7)	96.23(8)
Fe(7)-N(7)	2.168(2)	Fe(7)-O(15)-Fe(8)	94.30(8)
Fe-O (nitrate)		**μ₃-O bridges**	
Fe(2)-O(17)	2.092(2)	Fe(8)-O(35)-Fe(9)	128.72(9)
Fe(4)-O(20)	2.151(2)	Fe(1)-O(35)-Fe(8)	124.98(9)
Fe(4)-O(21)	2.263(2)	Fe(1)-O(35)-Fe(9)	101.11(8)
Fe(6)-O(23)	2.136(2)	Fe(2)-O(36)-Fe(10)	128.29(9)
Fe(8)-O(27)	2.132(2)	Fe(1)-O(36)-Fe(10)	121.61(9)
Fe(8)-O(26)	2.233(2)	Fe(1)-O(36)-Fe(2)	98.06(7)
Fe(9)-O(30)	2.124(2)	Fe(2)-O(37)-Fe(8)	126.13(9)
Fe(9)-O(29)	2.249(2)	Fe(3)-O(37)-Fe(8)	122.99(9)
Fe(10)-O(32)	2.155(2)	Fe(2)-O(37)-Fe(3)	96.21(7)
Fe(10)-O(33)	2.230(2)	Fe(4)-O(38)-Fe(8)	127.83(9)
		Fe(4)-O(38)-Fe(7)	123.94(9)
Fe-O (μ₃-O/OH)		Fe(7)-O(38)-Fe(8)	99.30(8)
Fe(9)-O(35)	1.951(2)	Fe(4)-O(39)-Fe(10)	128.41(9)
Fe(1)-O(35)	1.933(2)	Fe(3)-O(39)-Fe(10)	124.22(9)
Fe(8)-O(35)	1.866(2)	Fe(3)-O(39)-Fe(4)	101.93(7)
Fe(1)-O(36)	2.015(2)	Fe(4)-O(40)-Fe(6)	125.50(9)
Fe(2)-O(36)	1.965(2)	Fe(4)-O(40)-Fe(5)	124.33(9)
Fe(10)-O(36)	1.952(2)	Fe(5)-O(40)-Fe(6)	98.18(7)
Fe(2)-O(37)	2.064(2)	Fe(6)-O(41)-Fe(9)	124.62(9)
Fe(3)-O(37)	2.048(2)	Fe(7)-O(41)-Fe(9)	124.14(9)
Fe(8)-O(37)	2.006(2)	Fe(6)-O(41)-Fe(7)	98.43(8)
Fe(4)-O(38)	1.878(2)	Fe(10)-O(42)-Fe(9)	127.95(9)
Fe(7)-O(38)	1.961(2)	Fe(5)-O(42)-Fe(9)	123.86(9)
Fe(8)-O(38)	1.910(2)	Fe(10)-O(42)-Fe(5)	100.23(8)
Fe(3)-O(39)	1.910(2)		

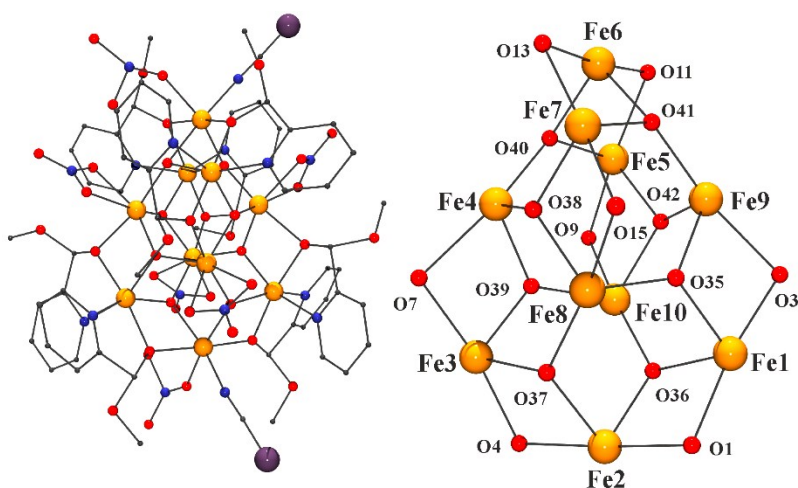|			
Fe(4)-O(39)	1.959(2)		
Fe(10)-O(39)	1.887(2)		
Fe(4)-O(40)	1.885(2)		
Fe(5)-O(40)	1.976(2)		
Fe(6)-O(40)	1.914(2)		
Fe(6)-O(41)	1.910(2)		
Fe(7)-O(41)	1.971(2)		
Fe(9)-O(41)	1.904(2)		
Fe(10)-O(42)	1.904(2)		
Fe(5)-O(42)	1.965(2)		
Fe(9)-O(42)	1.884(2)		

Fig. S3. A view of the molecular structure of cluster **1** (left) and its labeled core (rigth) from the partial resolution of the structure..

Table S3. Selected bond distances and angles for the Fe-O (μ_3-O/OH) core of compound **1** from the partial resolution of the structure.

Distance (Å)		Angle (deg.)	
Fe(9)-O(35)	1.922(5)	Fe(8)-O(35)-Fe(9)	128.9(3)
Fe(1)-O(35)	1.994(6)	Fe(1)-O(35)-Fe(8)	125.6(3)
Fe(8)-O(35)	1.846(6)	Fe(1)-O(35)-Fe(9)	98.8(3)
Fe(1)-O(36)	1.948(5)	Fe(2)-O(36)-Fe(10)	129.1(3)
Fe(2)-O(36)	1.931(5)	Fe(1)-O(36)-Fe(10)	125.8(3)
Fe(10)-O(36)	1.909(5)	Fe(1)-O(36)-Fe(2)	100.8(2)
Fe(2)-O(37)	2.185(6)	Fe(2)-O(37)-Fe(8)	125.7(3)
Fe(3)-O(37)	2.067(6)	Fe(3)-O(37)-Fe(8)	121.1(3)
Fe(8)-O(37)	2.042(6)	Fe(2)-O(37)-Fe(3)	95.8(2)
Fe(4)-O(38)	1.880(6)	Fe(4)-O(38)-Fe(8)	129.4(3)
Fe(7)-O(38)	1.964(6)	Fe(4)-O(38)-Fe(7)	123.9(3)
Fe(8)-O(38)	1.897(5)	Fe(7)-O(38)-Fe(8)	100.5(3)
Fe(3)-O(39)	1.905(6)	Fe(4)-O(39)-Fe(10)	129.2(3)
Fe(4)-O(39)	1.929(6)	Fe(3)-O(39)-Fe(10)	123.6(3)
Fe(10)-O(39)	1.907(6)	Fe(3)-O(39)-Fe(4)	102.4(3)
Fe(4)-O(40)	1.946(6)	Fe(4)-O(40)-Fe(6)	127.7(3)
Fe(5)-O(40)	1.997(7)	Fe(4)-O(40)-Fe(5)	123.2(3)
Fe(6)-O(40)	2.000(6)	Fe(5)-O(40)-Fe(6)	99.5(3)

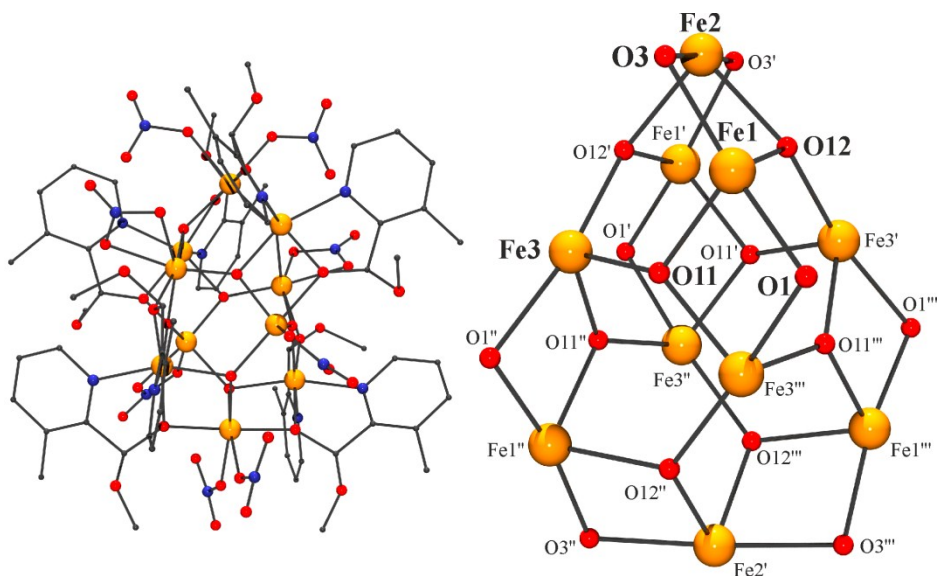|			
Fe(6)-O(41)	2.102(6)	Fe(6)-O(41)-Fe(9)	125.4(3)
Fe(7)-O(41)	2.059(6)	Fe(7)-O(41)-Fe(9)	124.1(3)
Fe(9)-O(41)	1.970(6)	Fe(6)-O(41)-Fe(7)	96.7(3)
Fe(10)-O(42)	1.909(6)	Fe(10)-O(42)-Fe(9)	126.9(3)
Fe(5)-O(42)	1.945(6)	Fe(5)-O(42)-Fe(9)	126.1(3)
Fe(9)-O(42)	1.872(6)	Fe(10)-O(42)-Fe(5)	101.0(3)

Fig. S4. A view of the molecular structure of cluster **3** (left) and its labeled core (rigth).

Table S4. Selected bond distances and angles for the core of compound **3**.

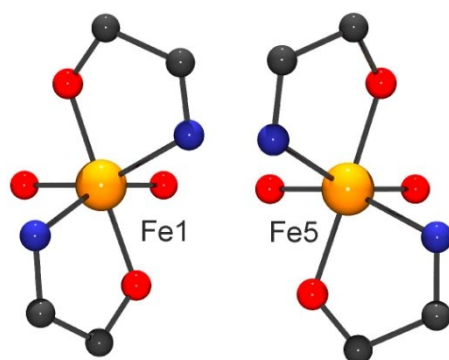| Fe-N		μ-O (from MeOhmp$^-$)	
Fe(1)-N(1)	2.126(10)		
Fe(1)-N(2)	2.161(9)	Fe(1)-O(3)-Fe(2)	98.7(5)
		Fe(1)-O(1)-Fe(3''')	95.7(4)
Fe-O (nitrate)			
Fe(2)-O(8)	2.064(14)	**Fe-O-Fe (μ_3-OH)**	
Fe(3)-(O5)	2.080(12)	Fe1-O(12)-Fe(2)	96.4(4)
Fe(3)-O(6)	2.226(12)	Fe1-O(12)-Fe(3')	122.8(5)
		Fe2-O(12)-Fe(3')	127.3(5)
Fe-O (μ_3-O)			
Fe(1)-O(11)	1.965(9)	**Fe-O-Fe (μ_3-O)**	
Fe(3)-O(11)	1.897(8)	Fe(1)-O(11)-Fe(3)	122.4(5)
Fe(3''')-O(11)	1.882(9)	Fe(1)-O(11)-Fe(3''')	100.8(4)
		Fe(3)-O(11)-Fe(3''')	130.5(5)
Fe-O (μ_3-OH)			
Fe(1)-O(12)	2.049(10)		
Fe(2)-O(12)	2.000(10)		
Fe(3')-O(12)	1.999(10)		

Fig. S5. A view of the Δ / Λ mirror image of the Fe^{III} cations linked to (*R*) or (*S*) enantiomers of MeO-pym$^-$ ligands.
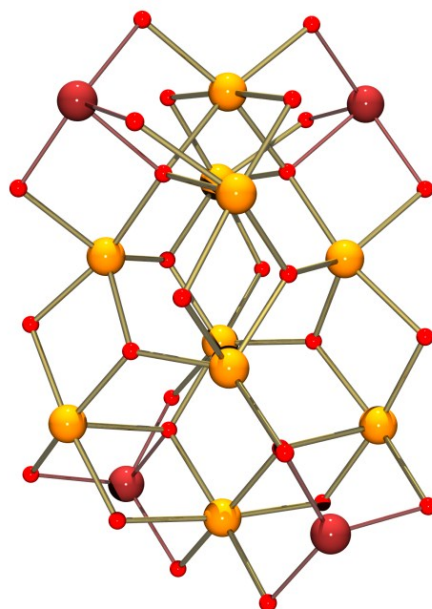

Fig. S6. Core of the two Fe_{14} clusters reported in references 18 and 19. These clusters show the same $\{Fe_{10}(\mu_3\text{-}O)_8\}$ inner core than complexes **1-3** (Fe^{III} cations in orange) with four additional Fe^{III} cations (red) keeping the S_4 symmetry.